ACS OMEGA

Open Access

http://pubs.acs.org/journal/acsodf

Article

Effects of Mini-Spidroin Repeat Region on the Mechanical Properties of Artificial Spider Silk Fibers

Benjamin Schmuck,* Gabriele Greco, Olga Shilkova, and Anna Rising*

Cite This: *ACS Omega* 2024, 9, 42423−42432

Read Online

ACCESS | Metrics & More | Article Recommendations | Supporting Information

ABSTRACT: Spiders can produce up to seven different types of silk, each with unique mechanical properties that stem from variations in the repetitive regions of spider silk proteins (spidroins). Artificial spider silk can be made from mini-spidroins in an all-aqueous-based spinning process, but the strongest fibers seldom reach more than 25% of the strength of native silk fibers. With the aim to improve the mechanical properties of silk fibers made from mini-spidroins and to understand the relationship between the protein design and the mechanical properties of the fibers, we designed 16 new spidroins, ranging from 31.7 to 59.5 kDa, that feature the globular spidroin N- and C-terminal domains, but harbor different repetitive sequences. We found that more than 50% of these constructs could be spun by extruding them into low-pH aqueous buffer and that the best fibers were produced from proteins whose repeat regions were derived from major ampullate spidroin 4 (MaSp4) and elastin. The mechanical properties differed between fiber types but did not correlate with the expected properties based on the origin of the repeats, suggesting that additional factors beyond protein design impact the properties of the fibers.

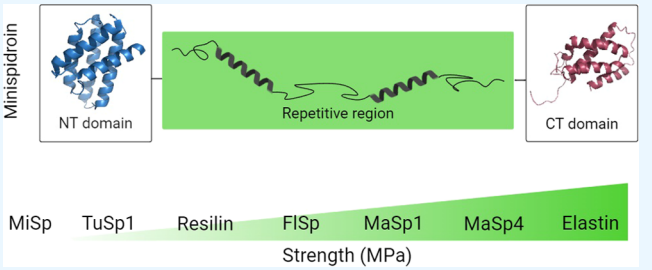

INTRODUCTION

Spider major ampullate silk is among the most impressive fibers known in terms of mechanical properties, which stem from a unique combination of high tensile strength and extensibility.[1−4] In addition, spiders make up to seven distinct types of silk,[5,6] each endowed with unique properties tailored to each type's specific function.[7,8] For instance, major ampullate silk possesses the highest strength and is used as a lifeline,[9] aciniform silk is more extensible and used for prey wrapping,[10] while flagelliform silk coated with aggregate glue is extremely extensible and hence used for making the capture spiral.[11]

All silk types are mainly composed of spider silk proteins (spidroins), which in general are very large with a molecular weight of up to 300 kDa.[12,13] The spidroins share a common architecture, featuring a repetitive (Rep) region, which is flanked by globularly folded N-terminal (NT)[14] and C-terminal (CT)[15] domains. NT and CT are responsible for the high solubility of the spidroins during storage and for polymerization of the spidroins when exposed to shear and a decreased pH.[15−19] The divergent mechanical properties of the silk fiber are likely to stem from disparities in the spidroins' Rep region.[20−22] For instance, the major ampullate spidroins (MaSps) carry characteristic poly-Ala blocks that alternate with Gly-rich regions,[23] and according to the current model of the fiber structure−function relationship, the poly-Ala form nanosized β-sheet crystals in the mature fiber conferring the fiber strength,[24] while the Gly-rich segments make up an amorphous and flexible matrix in which these crystals are embedded.[25,26] Another example comes from the flagelliform silk which is composed of spidroins that have Pro-rich repeat regions, which are believed to contribute to the extreme extensibility of this silk type.[27] Nevertheless, recent results suggest that this correlation is not straightforward, but that a combination of spidroins and other proteins is necessary to obtain the strength and extensibility of major ampullate silk.[28]

In the same way that spiders use their different silk types for specific purposes,[29] fibers with different properties are needed for specific industrial applications. For instance, an important selection criterion of fibers for clothing is comfort,[30,31] while sports goods could benefit from lightweight, elastic, and tough fibers.[32] The diverse and unique properties of spider silks make the material attractive for many applications, for instance, biomedical[33−36] and aerospace[37] applications, as durable components in robotics,[38] as sustainable wearables,[39] in sports goods,[40] and in other high-end textiles.[8,41]

Most artificial silk fibers are made from recombinant spidroin-like proteins that often consist of the Rep unit alone (no terminal domains). Fibers produced from large Rep proteins (300 kDa[42−44]) can feature GPa strength.[43,44]

Received: June 29, 2024
Revised: August 19, 2024
Accepted: September 19, 2024
Published: October 7, 2024

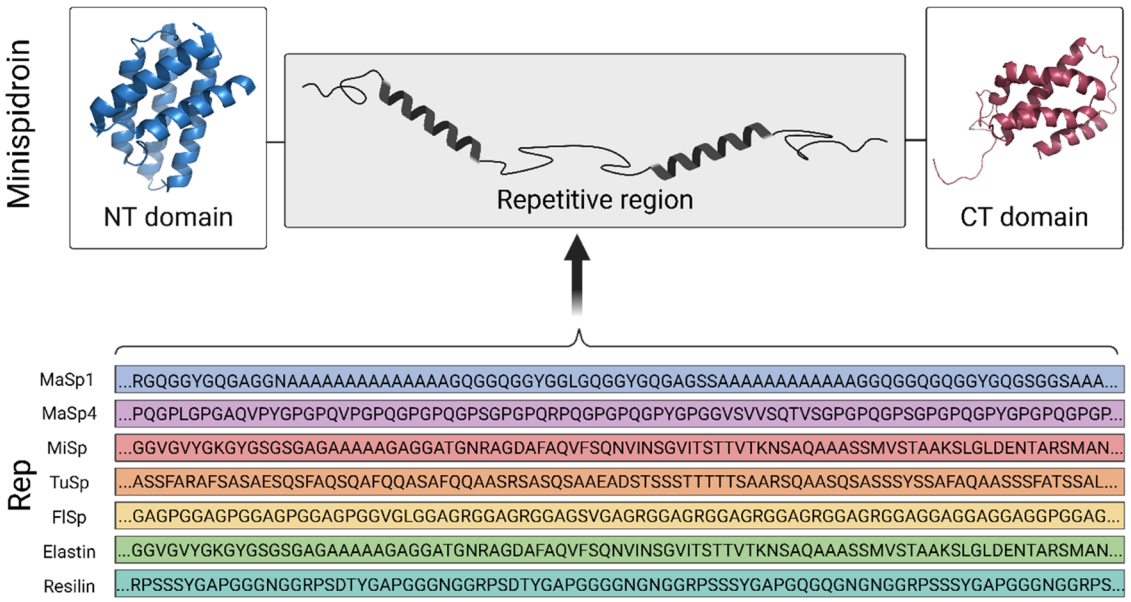

Figure 1. Using the basic mini-spidroin concept described by Andersson et al.,[45] the Rep region in NT2RepCT was replaced with other natural and engineered repeats. Altogether 16 proteins were designed (listed in Table 1) with Rep regions originating from MaSp1 (three different constructs with an increased size of the Rep region and two with shortened poly-Ala blocks), MaSp4 (two constructs), elastin (two constructs), FlSp (two constructs), TuSp (two constructs), resilin (one construct), and MiSp (one construct). Examples of Rep regions are shown in the lower panel, the complete sequences of NT, CT, and all Rep regions are listed in Table S1, and a short description of each insert is provided in Table S2. The figure was made with Biorender.com using structures from Protein Data Bank (PDB)2MFZ and 4FBS.

Table 1. List of Mini-Spidroins Studied in This Work[a]

strategy	construct	length of rep (# aa)	M_w (kDa)	solubility after cell lysis	yield after purification (mg/L)*	spinnability
control	NT2RepCT	77	33.2	+++	250[52]	++
	$(A_3I)_3$-A_{14}	77	33.3	+++	207[52]	−
poly-Ala length	MaSp1_A_4	56	31.7	+++	209	+
	MaSp1_A_8	64	32.2	+++	170	−
MaSp1 length	MaSp1_110	110	35.7	+++	183	++
	MaSp1_173	173	40.7	n.a	0	n.a
	MaSp1_237	237	45.8	n.a	0	n.a
spidroin types	MaSp4_125	125	38.2	+++	231	++
	MaSp4_175	175	42.8	+++	80	++
	MaSp4_252	252	49.7	++	98	−
	MiSp_206	206	42.1	+++	114	++
	FlSp_132	132	36.8	++	157	++
	FlSp_232	232	44.7	+++	61	−
	TuSp1_174	174	43.2	+++	114	++
	TuSp2_345	345	59.5	+++	35	−
natural repeats	Resilin_142	142	39.5	++	48	++
	Elastin_116	116	36.5	+++	88	++
	Elastin_221	221	45.5	++	26	−

[a]A compilation of 18 mini-spidroins including two previously characterized proteins (NT2RepCT[51,53,54] and $(A_3I)_3$-A_{14}[52]). Expression values for NT2RepCT and $(A_3I)_3$-A_{14} were reported earlier by Arndt et al.[52] *Average of a 10 × 1L cultures. Solubility after cell lysis was rated according to the following thresholds: + ++ almost all; + + more than 50%; + less than 50%; − not soluble; n.a. since no protein was expressed. The spinnability of the different constructs was rated as − not spinnable in that fibers were weak and fractured either when the fiber exited the capillary or while picking it up from the bath and guiding it to the collection wheel. + Spinnable, but discontinuous. To collect enough fibers for tensile testing, the fiber had to be picked up several times and guided to the collection wheel. + + Continuous spinning. The fiber was picked up and continuously collected for 1−2 min yielding up to 60 m of fiber, before the process was aborted to ensure evenly spaced fibers on the collection wheel.

However, this production method comes with the disadvantage that solvents such as hexafluoropropanol and methanol are needed during the spinning process and that the protein yield is rather low. Another strategy for producing artificial spider silk is to express natively folded mini-spidroins that consist of the NT, a short Rep, and a CT.[45−50] The advantage of this approach is that the proteins can be purified using native conditions, and the artificial silk fibers are formed by decreasing the pH and/or using shear forces.[45−50] This strategy, on the other hand, comes with the disadvantage that fibers are weaker, reaching a maximum strength of 250 MPa.[48,51] One explanation for the reduced strength compared to the non-native spinning methodology could be the

https://doi.org/10.1021/acsomega.4c06031
ACS Omega 2024, 9, 42423−42432

Table 2. Mechanical Properties of Spinnable Constructs in Order according to the Strength[a]

construct	diameter (μm)	strain at break (%)	eng. strength (MPa)	Young's modulus (GPa)	toughness modulus (MJ m^{-3})
MiSp_206	11.8 ± 0.6	93% ± 43%	74 ± 8	2.5 ± 0.4	59 ± 27
MaSp1_A_4	17.7 ± 6.3	6% ± 2%	75 ± 28	2.0 ± 1.0	2 ± 1
TuSp1_174	19.8 ± 3.4	6% ± 2%	76 ± 19	2.3 ± 0.6	3 ± 1
Resilin_142	13.5 ± 3.9	21% ± 26%	97 ± 18	2.7 ± 0.8	17 ± 24
FlSp_132[b]	9.9 ± 3.0	93% ± 43%	98 ± 38	2.7 ± 0.8	74 ± 49
MaSp1_110	9.7 ± 1.7	106% ± 32%	105 ± 25	2.6 ± 0.9	75 ± 23
NT2RepCT[a]	8.8 ± 2.7	113% ± 28%	110 ± 30	2.2 ± 0.6	90 ± 30
MaSp4_125[b]	9.0 ± 2.9	89% ± 26%	134 ± 38	2.4 ± 0.6	84 ± 35
MaSp4_175	9.8 ± 2.5	83% ± 31%	143 ± 78	3.3 ± 1.6	96 ± 61
Elastin_116[b]	9.8 ± 2.9	105% ± 32%	143 ± 32	2.9 ± 1.1	109 ± 47

[a]For each construct, at least 10 fibers were tensile tested. Outliers were not removed. The values reported after ± represent one standard deviation. Representative stress−strain curves are shown in Figure S2. [a]Added for comparison purposes where the values represent the average from 89 fibers tensile tested that originate from 8 different spinning occasions, as reported in Schmuck et al.[51] [b]The values are averages of fibers made from two or more spinning occasions and tensile testing of more than 20 fibers. A graphical representation and statistical significance compared to NT2RepCT is shown in Figure S4. Representative stress−strain curves for all fiber types, except for NT2RepCT, are shown in Figure S5. Representative stress−strain curves for NT2RepCT are shown in Schmuck et al.[51]

comparatively small size of the mini-spidroins of less than 100 kDa.[46−49,51,52]

With the aim to improve and specifically tailor the mechanical properties of artificial silk fibers made from mini-spidroins and to understand the relationship between the protein design and the mechanical properties of the fibers, we systematically modified the mini-spidroin NT2RepCT. NT2RepCT has a Rep from MaSp1 featuring two poly-Ala blocks located between NT and CT, expresses at high very yields of up to 21 g/L with *Escherichia coli*,[53] and is extremely soluble in aqueous buffers (500 mg/mL).[54] To modify NT2RepCT, we explored four different strategies: (1) to vary the poly-Ala segment length, (2) to increase the size of the MaSp1 region, (3) to insert Rep segments from different spidroin types, and (4) to insert Rep segments from other naturally occurring fibrous proteins. Thus, a battery of 16 mini-spidroins was designed (Figure 1), and fibers spun from these proteins were characterized by determining their mechanical properties.

RESULTS AND DISCUSSION

Expression and Purification. In total, we designed 16 constructs that carry different Rep regions inserted between the terminal domains (complete sequences are listed in Tables S1 and S2). Three of these carried Rep regions from the MaSp1 from *Euprosthenops australis*, three from a MaSp4 from *Caerostris darwini*,[55] two from elastin from *Homo sapiens*, two from a tubuliform spidroin (TuSp) from *Trichonephila clavipes*,[56] two from a flagelliform spidroin (FlSp) from *T. clavipes*,[56] one from resilin from *Drosophila simulans*,[57] and one from minor ampullate spidroin (MiSp) from *Araneus ventricosus*.[58] These proteins were named after the protein from which the repetitive segment was derived and the number of amino acid residues in the repeat region. Two additional constructs were based on the MaSp1 Rep region, in which the natural 15 and 14-residue-long poly-Ala stretches were replaced by four or eight consecutive Ala residues, which were named MaSp1_A_4 and MaSp1_A_8, respectively. As reference, already reported values for solubility and yield of the previously characterized NT2RepCT[51,53,54] (according to the nomenclature described herein, NT2RepCT would be called MaSp1_77) and $(A_3I)_3$-A_{14}[52] proteins were used.

Most constructs expressed well and were soluble after cell lysis in a Tris-HCl buffer, reaching yields after purification of 26 and 250 mg/L in shake flask cultivations (Table 1 and Figure S1). Overall, lower yields after purification were obtained for mini-spidroins that carried longer Rep regions compared to shorter variants (Figure S2). This is in line with previous publications[46−48] and could be due to the inability of the prokaryotic translational machinery to cope with the high demands of specific amino acid residues,[42] increased aggregation propensity of long repetitive proteins, toxicity of the expressed proteins, and/or unfavorable secondary structure formation of the repetitive mRNAs.[59]

Spinning of Artificial Spider Silk. The mini-spidroins that could be isolated in a soluble form were concentrated and subjected to spinning using a protocol developed for NT2RepCT.[51] This protocol is purely aqueous-based but differs slightly compared to previous studies published by our group[52,54] in terms of buffer in the coagulation bath, reeling speed, and the tip diameter of the capillary used for extrusion of the spinning dope (see the Materials and Methods section for details). Using these spinning conditions, the different mini-spidroins were characterized as being continuously spinnable, discontinuous, or not spinnable. Spinnable fibers could be guided through the bath and collected onto a wheel rotating at 36 m/min. Some mini-spidroins formed fibers that were too fragile to be collected onto the rotating wheel and were then categorized as nonspinnable. Of the 18 mini-spidroin variants (16 novel + 2 controls), 10 were possible to spin into continuous fibers, seven were nonspinnable, and one type could be collected onto the wheel, but the spinning was not continuous (Table 1).

Mini-Spidroins with Different Lengths of the Poly-Ala Blocks. The poly-Ala blocks found in the MaSp Rep region form crystals in the fiber, which are believed to confer the strength of the fibers. Molecular simulations have suggested that restricting the size of the crystals is imperative for optimizing the strength since large crystals will be more likely to bend and fracture than smaller ones.[24,60] At the same time, poly-Ala stretches composed of less than seven residues are not expected to form β-sheet crystals.[61] To build on these results, Hu and co-workers investigated recombinant spidroins containing 5, 8, or 12 Ala residues in the poly-Ala motif.[62] They found that the construct containing 12 Ala residues

https://doi.org/10.1021/acsomega.4c06031
ACS Omega 2024, 9, 42423−42432

produced artificial silk fibers that were weaker compared with the other constructs. The eight Ala spidroin produced the strongest (623 MPa) and toughest (107 MJ m^{-3}) artificial silk fibers. Accordingly, we designed two variants of NT2RepCT in which the poly-Ala blocks were shortened to eight or four residues, respectively (MaSp1_A_8 and MaSp1_A_4). Surprisingly, MaSp1_A_8 was not spinnable, as fibers broke when guided through the spinning bath. Likewise, it was difficult to spin and collect MaSp1_A_4 fibers, which is reflected in the mechanical properties of these fibers which were among those with the lowest strength and extensibility of all fibers investigated herein (Table 2). Hence, reducing the number of Ala residues in the poly-Ala motif of NT2RepCT did not lead to improvement of the fibers' mechanical properties.

MaSp1 Mini-Spidroins with Different Lengths of the Rep Region. To investigate the impact of longer repeat regions, we extended the repeat region of NT2RepCT so that the resulting mini-spidroins encompassed three poly-Ala blocks (MaSp1_110), five poly-Ala blocks (MaSp1_173), or seven poly-Ala blocks (MaSp1_237). We first assessed the expression levels and benchmarked against NT2RepCT that can be expressed and purified at high yields reaching 250 mg/L in shake flask cultivations.[52,54] From shake flask cultures, MaSp1_110 can be obtained at 183 mg/L, but surprisingly, we could not identify the longer MaSp1_173 and MaSp1_237 on an SDS-PAGE of the cells after expression (Figure S3), which indicates a very low or nonexisting expression. Interestingly, others such as Heidebrecht and co-workers succeeded in expressing constructs having 24 poly-Ala blocks with a standard *E. coli* strain, showing that it is in principle possible to recombinantly express spidroins with longer Rep.[63] In this particular example, each poly-Ala block hosted only 5 Ala residues, which is much fewer compared to the up to 15 consecutive Ala residues found in our MaSp1 Rep segment. Nevertheless, we believe that the longer poly-Ala block is probably not the only cause for the failed expression of MaSp1_173 and MaSp1_237, since a recent study by Hu et al. succeeded to express spidroins having 13 repeats where each repeat hosted a block of 12 Ala residues with an expression level of 2.5 g/L using a bioreactor.[62] As far as we could judge, the authors in the two examples did not use any additional vectors during expression with *E. coli* to elevate the alanyl- or glycyl-tRNA pool.[42] An additional factor that could explain the loss of expression would be if the longer mini-spidroin variants are toxic to the bacteria, but the exact reason for the abrupt drop in protein expression is not known. The expression system presented here could potentially be improved by screening different bacterial strains and promotors, using a different codon optimization strategy, and possibly also by designing different mini-spidroin variants.

Next, we attempted to spin fibers from MaSp1_110, which was successful. The mechanical characterization of these fibers showed no significant difference compared to that of NT2RepCT fibers (Table 2 and Figure S4). This may be a result of that the MaSp1_110 Rep region is not long enough to mediate a significant impact on fiber mechanical properties.

In theory, longer repeat regions should result in an increased number of intermolecular interactions and, thereby, stronger fibers. In line with this, several reports in the scientific literature investigated this aspect, applying all-aqueous and native conditions for expression, purification, and spinning without the use of denaturing agents in any step of the process. Zhou et al.[48] found a strong dependency of strength and size when inserting aciniform spidroin repeat segments into a mini-spidroin. When such a small mini-spidroin was spun (45.8 kDa), the resulting fibers had a strength of 52 MPa, but when the repetitive segment was extended, which resulted in a 104 kDa construct, the resulting fibers had a strength of 245 MPa. Even though these results are quite impressive, the expression was overall low, and the larger 104 kDa variant was not soluble in aqueous buffers. In a follow-up study, 44 and 96 kDa recombinant spidroins with repeats from FlSp were spun into fibers. Interestingly, despite the relatively large difference in molecular weight, the fiber strength was moderately increased from 182 to 253 MPa using larger spidroins. At the same time, these fibers were rather brittle with a strain at break of 12%, which is surprising considering the impressive extensibility of the flagelliform silk.[46] In the literature, there are also conflicting reports regarding the relationship between M_w and the mechanical properties of the fibers. In a study where spidroins containing different lengths of the MaSp1 repeat region were spun into fibers, the largest constructs (60.8 kDa) gave inferior fibers compared to a 42.5 kDa variant, which could be spun into a fiber with a strength of 149 MPa.[47] The emerging inconclusive picture of the effect of longer Rep segments on the mechanical properties could be a result of numerous parameters, which are discussed further below.

Since we were unsuccessful in expressing the mini-spidroins based on MaSp1 from *Euprosthenops australis* with repeat regions exceeding 110 residues, we attempted to produce longer variants with repeats originating from other spidroins.

Mini-Spidroins with Rep Regions from Different Spidroin Types. The mechanical properties of different spider silks vary significantly, and this is related to differences in the primary structure of the Rep region.[22,64] As mentioned before, the major ampullate silk, made up primarily of MaSps,[65,66] is the strongest of the different silks.[67] The MaSp4 has been identified in the spider species *Caerostris darwini*[55,68] and *Araneus ventricous*[69] and has been associated with an increased extensibility of the fiber.[55] To examine the influence of MaSp4 Rep on our artificial silk is especially interesting because this spidroin type has been scarcely studied. MiSps are the main constituents of the minor ampullate silk, which have a lower tensile strength than major ampullate silk, but increased extensibility. Flagelliform silk stands out as the most extensible fiber (>200%) of all of the different silk types which relates to the Pro-rich repeat region of the FlSps, while tubuliform silk is intermediate in terms of both strength and strain.[67] Thus, we expected that the insertion of different Rep between NT and CT would make the artificial silk fibers substantially different compared to reference NT2RepCT fibers, even more so as we have previously seen a drastic effect by introducing only very few mutations in the Rep of NT2RepCT.[52]

The new mini-spidroins containing Rep from different spidroin types could all be successfully spun into fibers (Table 2), except for constructs having more than 220 residues in Rep (FlSp_232, MaSp4_252, and TuSp2_345). The longest constructs were classified as not spinnable because the fibers were too fragile to be collected or because of aggregate formation in the spinning dope, as in the case of TuSp2_345, for which extrusion was inhibited due to clogging. Among the eight mini-spidroin variants with Rep regions from different spidroin types, only MaSp4_125 and MaSp4_175 were significantly stronger. These fibers had an average strength of 134 and 143 MPa, respectively, compared to 110 MPa for

https://doi.org/10.1021/acsomega.4c06031
ACS Omega 2024, 9, 42423−42432

NT2RepCT (Table 2 and Figure S4). Since NT2RepCT, MaSp4_125, and MaSp4_175 have similar M_w and identical terminal domains, the increase in strength could be related to the nature of the MaSp4 repeat. The results are surprising since the MaSp4 is Pro-rich and void of poly-Ala blocks, which should give a more extensible fiber according to the current structure−function models. Fibers obtained from the mini-spidroin constructs MiSp_206, and TuSp_174 were significantly weaker. The strain at break for all constructs with Rep from different spidroins was above 83%, which is comparable to NT2RepCT fibers. An exception is the construct TuSp1_174 which resulted in brittle fibers. In summary, we did not achieve mechanical properties that correlated to the behavior of the native silk fibers that the respective repeats were derived from, and moreover, the mechanical properties of the fibers made from the new mini-spidroins were very similar to the mechanical properties of NT2RepCT fibers.

Mini-Spidroins with Rep Regions from Other Fibrous Proteins. In nature, the elastomers tropoelastin and resilin stand out as examples of proteins that are found in tissues with impressive mechanical properties. Tropoelastin is found in connective tissues and is cross-linked via Lys residues into elastin.[70] Silk-elastin hybrid materials are frequently described in the literature in the context of making biomaterials, for instance, to assemble tissue scaffolds by electrospinning,[71] to tune the mechanical properties of hydrogels,[72] and for modulating the self-assembly kinetics of silk/elastin hybrids to make nanomaterials.[73] Herein, we could efficiently produce and spin fibers from a 36.5 kDa silk-elastin hybrid protein (Elastin_116), but the longer variant of this protein (Elastin_221) could not be spun into continuous fibers, as was also the case for the longer constructs with Rep from other spidroins. Notably, the fibers spun from Elastin_116 proteins were the toughest among all fibers investigated herein, reaching 143 MPa in strength, a strain at break of 105%, a Young's modulus of 2.9 GPa, and a toughness modulus of 109 MJ/m^3.

Resilin is found in elastic tissues of insects and arthropods and the proteins are cross-linked via Tyr residues.[74,75] Resilin and resilin/silk hybrids have been mainly investigated for their use as biomaterials,[76] but there are also attempts to increase the mechanical properties of silkworm silk by inserting the resilin gene into the silkworm genome.[77] In our hands, fibers made from a mini-spidroin carrying Rep from Resilin (Resilin_142) could be continuously spun. The strength of Resilin_142 fibers was within the experimental error compared to NT2RepCT fibers, but the strain at break was significantly reduced (Figure S4 and Table 2).

To our knowledge, there are no previous examples of silk-elastin or silk-resilin hybrid proteins that have been continuously wet-spun into macroscopic fibers. Silk-resilin/elastin hybrid proteins could in theory harness the high deformability and resilience of the respective natural materials, but to achieve this, we likely have to find ways to allow the repeat regions to fold properly and to achieve the intermolecular cross-links that are present in the native materials.

Control Proteins. As already mentioned before, the spinning condition used in this study were optimized for NT2RepCT[51] and have not been tested on the engineered variant $(A_3I)_3$-A_{14}, which has been shown to form fibers that are as tough as native spider silk in a recent study.[52] Interestingly, the $(A_3I)_3$-A_{14} was in this study categorized as nonspinnable and is therefore not listed in Table 2, because the fiber broke as soon as it was placed on the collection wheel. This is likely due to that the spinning conditions used herein were different from those in Arndt et al.[52] Specifically, the glass capillaries used in the current study had a larger opening, the spinning bath did not contain NaCl, and the speed of collection was much faster. These results attest to previously published notions, that in order to achieve the best possible mechanical properties of a fiber spun from a specific mini-spidroin, the spinning conditions need to be screened and optimized systematically.[51] However, performing such large screens for the relatively large number of proteins investigated herein would require several years' work.

General Discussion. The main intention of the present study was to investigate if and how different primary structures of the Rep region in mini-spidroins affect the mechanical properties of artificially spun spider silk when using all-aqueous spinning conditions. To our surprise, the strength of all as-spun fibers using identical spinning conditions was found to be within a rather narrow range of 74−143 MPa. Interestingly, the only constructs that were better in terms of strength compared to the control mini-spidroin NT2RepCT (MaSp1_77) are constructs based on MaSp4 (up 143 MPa)[55] and elastin (143 MPa) (Table 2). None of the fibers developed herein had a higher strain at break than the control NT2RepCT (113%), but the majority of the constructs (73%) resulted in fibers with a strain at break above 50%. Only the MaSp1_A_4 and TuSp1_174 fibers failed at the yielding point. The fiber with the highest strength that was significantly different compared to NT2RepCT was made from Elastin_116. The strain at break values of NT2RepCT and Elastin_116 fibers were comparable, as was the toughness modulus (Figure S4). We therefore conclude that the mechanical properties of fibers spun from mini-spidroins with diverse primary structures in their repeat regions are surprisingly similar. The relatively small improvements we could achieve in this cohort of proteins are in the range that can be achieved when changing the spinning conditions.[51]

The question remains why most mini-spidroins investigated in this study did not give rise to fibers with more diverse mechanical properties and failed to reflect the properties of the respective native silk fibers. One explanation for this observation could be that the spinning conditions were not optimized for the respective construct, which could have substantially different optima concerning the buffer type, buffer concentration, pH, extrusion rate, and dope concentration. The biology of all glands, except the major ampullate gland, remains largely unexplored, which means that there may be unknown conditions or components that are important for the correct polymerization of a specific silk type. Specifically, several studies have shown that there are several nonclassical spider silk proteins in the major ampullate silk, all of which have unknown functions.[65,66,78] These proteins and the combination of different proteins could potentially be important for the mechanical properties. However, even though the presence of other spidroins and nonspidroins should not be neglected,[65,66] the bulk of each fiber type is made from the corresponding spidroin type,[66] and thus they should be a main contributor to the mechanical properties. Another factor to take into account could be that the spidroin terminal domains may have evolved to function optimally with a specific repeat, which could also influence the results as we used the same NT and CT in all protein constructs. Yet

https://doi.org/10.1021/acsomega.4c06031
ACS Omega 2024, 9, 42423−42432

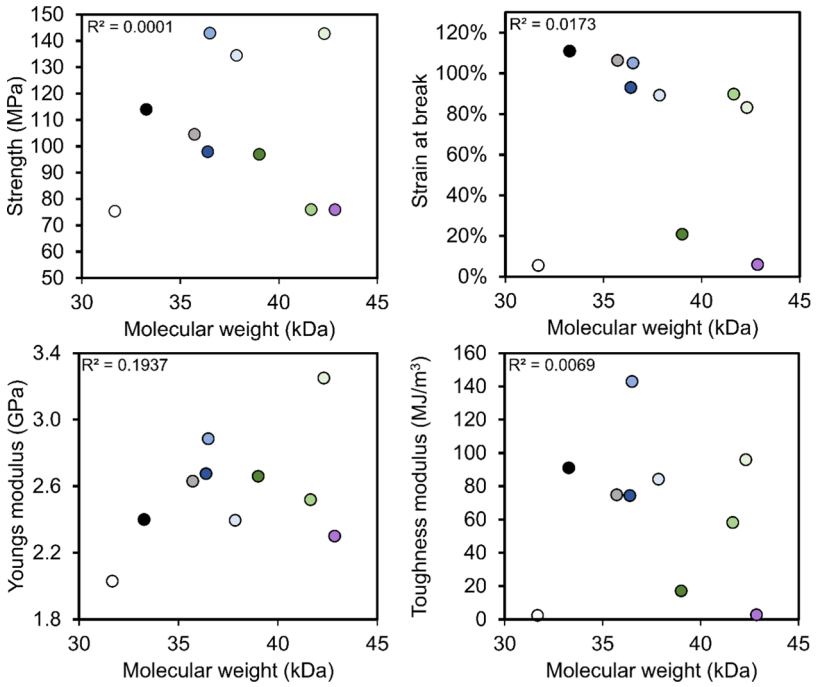

Figure 2. Mechanical properties for artificial silk fibers plotted against the molecular weight of the mini-spidroins used in this study. The different colors of the circles are used to represent the different mini-spidroins where white represents MaSp1_A_4, black NT2RepCT, gray MaSp1_110, dark blue FlSp_132, blue Elastin_116, light blue MaSp4_125, dark green Resilin_142, green MiSp_206, light green MaSp4_175, and purple TuSp1_174. R^2 was obtained by least-squares regression.

another contributing factor could be that the repeat regions affect the ability of the mini-spidroins to form liquid−liquid phase-separated (LLPS) droplets before polymerization, which has been suggested to be an important step in the spinning process and deserves further investigation.[50,79−82] Moreover, shear forces are important for alignment and to induce the formation of β-sheets,[83] but the extrusion of the spidroins through the glass capillary used herein may not be enough to align the larger spidroins, thus causing a suboptimal arrangement and as a consequence a weaker fiber is obtained. The significantly smaller size of the mini-spidroins compared to the native spidroins could of course also affect the properties of the fiber if they are too short to form correct intermolecular interactions (Figure 2). When using denaturing conditions for the preparation of the spinning dope, the literature suggests that spidroins with an M_w comparable to native spidroins (up to 300 kDa) are required for making fibers with a strength of 1 GPa.[42,43,63,84] Considering this, it may not be too surprising that we could not improve the strength more by spinning longer proteins, as the largest spinnable spidroin in this study had an M_w of only 43 kDa. Although our results suggest that there is no correlation between strength and molecular weight (Figure 2), it should be noted that molecular weight difference between the smallest and largest spidroin is only 37%, which may be too little to detect effects of protein molecular weight.

CONCLUSIONS

We have shown that the basic NT-Rep-CT construct can host a broad range of different amino acid sequences in the Rep region and still maintain the ability to be spun into continuous fibers in our all-aqueous spinning system. Interestingly, we show that the primary structure of the Rep has a rather moderate influence on the resulting fibers' mechanical properties, at least for repeat regions ranging from 32 to 43 kDa. We also found that spidroins with a molecular weight >45 kDa were difficult to spin in the spinning setup used in this work. Moving forward, optimizing protein design, spinning methodologies, and postprocessing techniques will be crucial for realizing the full potential of artificial spider silk in various applications.

MATERIALS AND METHODS

Cloning and Protein Expression. Synthetic fragments were cloned in the pT7-His_6-NT-CT vector between *Eco*RI and *Bam*HI sites. Resulted construct was transformed in BL21(DE3) *E. coli*, and the positive colonies were sequenced before preparing a glycerol stock, which was stored at −80 °C. For protein expression, LB broth medium containing kanamycin (70 μg/mL) was first inoculated with a glycerol stock of the previously transformed *E. coli* and then incubated overnight at 30 °C while shaking at 250 rpm. The overnight culture was used for inoculation of up to 10 × 1 L of fresh LB media also containing 70 μg/mL kanamycin. Then, the cultures were incubated at 30 °C with shaking (110 rpm) until OD_{600} reached 0.6, after which the temperature was lowered to 20 °C and protein expression was induced at OD_{600} 0.8 by adding isopropylthiogalactoside to a final concentration of 0.15 mM. The cells were cultured overnight at 20 °C with shaking (110 rpm) and were then harvested by centrifugation for 20 min at 5000*g* at 4 °C. The pellets were resuspended in 20 mM Tris pH 8 and stored at −20 °C.

Protein Purification. Lysis was performed in a cell disrupter (T-S Series Machine, Constant Systems Limited) at 30 kPsi, after which the lysate was centrifuged at 25 000*g* at 4 °C for 30 min. The supernatant was loaded on 2 sequentially connected 20 mL of HisPrep FF16/10 (Cytiva) columns, washed with 5 CV 20 mM Tris-HCl pH 8.0 and 5 CV 2 mM imidazole in 20 mM Tris-HCl pH 8.0. The protein was eluted

https://doi.org/10.1021/acsomega.4c06031
ACS Omega 2024, 9, 42423−42432

with 200 mM imidazole in 20 mM Tris-HCl pH 8.0. The eluted protein was dialyzed against 20 mM Tris (pH 8.0) at 4 °C overnight using a Spectra/Por dialysis membrane with a 6−8 kDa molecular-weight cutoff. SDS−PAGE (4−20%) and Coomassie Brilliant Blue staining were used to determine the purity of the protein. Broad Range Protein Ladder (Thermo Fisher Scientific) was used as a size standard. Protein concentration was determined by recording the absorbance of a 10-diluted dialyzed eluate at 280 nm.

Preparation of the Spinning Dope. Purified protein was concentrated to ∼300 mg/mL with an Amicon Ultra-15 centrifugal filter unit (Merck-Millipore, Darmstadt, Germany) equipped with an ultracel-10 membrane (10 kDa cutoff) at 4000*g* and 4 °C to prepare the spinning dope. The concentration of the concentrated protein was determined by recording the absorbance at 280 nm of a 500 × diluted sample, in triplicate, before the spinning dope was transferred to a 1 mL syringe with a Luer lock (BD, Franklin Lakes, New Jersey), and stored at −20 °C.

All-Aqueous Spinning of Artificial Silk Fibers. The all-aqueous spinning of the protein concentrate (spinning dope) was performed according to a method described by Andersson et al.[45] and fine-tuned by Schmuck et al.[51] Briefly, the spinning dope was thawed at room temperature, and the 1 mL syringe was connected to a pulled glass capillary with a tapered opening of 40−100 μm (G1 Narishige, Tokyo, Japan with an O.D. of 1.0 mm and μD of 0.6 mm, pulled using a Micro Electrode Puller, Stoelting Co. 51217, Wood Dale, Illinois). Then, the syringe was placed into a neMESYS low-pressure (290 N) syringe pump (Cetoni, Korbußen, Germany). Using a flow rate of 17 μL/min, the dope was extruded through the glass capillary into an 80 cm long coagulation bath containing 0.75 M acetate buffer (pH 5). If possible, the fiber was collected continuously at the end of the bath, using a rotating wheel, with a circumference of 35 cm, and a reeling speed of 59 cm s^{-1}, at a relative humidity (RH) of <40%.

Tensile Testing. Tensile testing was conducted with an Instron 5943 equipped with a 5N load cell. The fibers were mounted in a 1 cm × 1 cm paper frame using double-sided tape (circa 1 cm gauge length). The diameter of the fibers was determined with light microscopy by measuring the diameter three times, in three arbitrary locations along the fiber. Then, the paper frame was mounted in the tensile tester using grips before cutting the sides of the paper frame. During the tensile test, a displacement speed of 6 mm/min was applied. All tensile tests were conducted at an RH below 40% and at a temperature of 22 °C. The average diameter was used to calculate the cross-sectional area assuming a round cross section, which likely underestimated the strength of the fibers by a factor of 1.8.[85] With the cross section and the gauge length, we calculated engineering stress and strain. The toughness modulus was calculated as the area under the stress strain curve and the Young's modulus as the slope in the initial linear elastic region of the stress strain curve.

■ ASSOCIATED CONTENT

Supporting Information

The Supporting Information is available free of charge at https://pubs.acs.org/doi/10.1021/acsomega.4c06031.

SDS-PAGE images highlighting the expression and purification process of the spidroins; graphical representation of the mechanical properties of the fibers; stress−strain curves, and sequence and a short description of the spidroins used in this study (PDF)

■ AUTHOR INFORMATION

Corresponding Authors

Benjamin Schmuck − *Department of Medicine Huddinge, Karolinska Institutet, Neo, 141 83 Huddinge, Sweden; Department of Animal Biosciences, Swedish University of Agricultural Sciences, 750 07 Uppsala, Sweden;* orcid.org/0000-0003-4021-6458; Email: benjamin.schmuck@ki.se

Anna Rising − *Department of Medicine Huddinge, Karolinska Institutet, Neo, 141 83 Huddinge, Sweden; Department of Animal Biosciences, Swedish University of Agricultural Sciences, 750 07 Uppsala, Sweden;* orcid.org/0000-0002-1872-1207; Email: anna.rising@ki.se

Authors

Gabriele Greco − *Department of Animal Biosciences, Swedish University of Agricultural Sciences, 750 07 Uppsala, Sweden;* orcid.org/0000-0003-3356-7081

Olga Shilkova − *Department of Medicine Huddinge, Karolinska Institutet, Neo, 141 83 Huddinge, Sweden*

Complete contact information is available at: https://pubs.acs.org/10.1021/acsomega.4c06031

Notes

The authors declare no competing financial interest.

■ ACKNOWLEDGMENTS

This work was supported by European Research Council (ERC) under the European Union's Horizon 2020 research and innovation program (grant agreement no. 815357), Knut and Alice Wallenberg Foundation to SciLife Lab for research in Data Driven Life Science (DDLS) KAW 2020.0239, the Center for Innovative Medicine (CIMED) at Karolinska Institutet and Stockholm City Council, FORMAS (2019-00427 and 2023-01313), Olle Engkvist stiftelse (207-0375 and 233-0334), and the Swedish Research Council (2019-01257). A.R. and G.G. were supported by Wenner-Gren stiftelse (UPD2021-0047). B.S. was supported by FORMAS (2023-00871). G.G. was supported by the project "EPASS" under the HORIZON TMA MSCA Postdoctoral Fellowships−European Fellowships (project number 101103616).

■ REFERENCES

(1) Agnarsson, I.; Kuntner, M.; Blackledge, T. A. Bioprospecting Finds the Toughest Biological Material: Extraordinary Silk from a Giant Riverine Orb Spider. *PLoS One* **2010**, *5* (9), e11234.

(2) Gosline, J. M.; Guerette, P. A.; Ortlepp, C. S.; Savage, K. N. The Mechanical Design of Spider Silks: From Fibroin Sequence to Mechanical Function. *J. Exp. Biol.* **1999**, *202* (23), 3295−3303.

(3) Vollrath, F.; Knight, D. P. Liquid Crystalline Spinning of Spider Silk. *Nature* **2001**, *410* (6828), 541−548.

(4) Arakawa, K.; Kono, N.; Malay, A. D.; Tateishi, A.; Ifuku, N.; Masunaga, H.; Sato, R.; Tsuchiya, K.; Ohtoshi, R.; Pedrazzoli, D.; Shinohara, A.; Ito, Y.; Nakamura, H.; Tanikawa, A.; Suzuki, Y.; Ichikawa, T.; Fujita, S.; Fujiwara, M.; Tomita, M.; Blamires, S. J.; Chuah, J. A.; Craig, H.; Foong, C. P.; Greco, G.; Guan, J.; Holland, C.; Kaplan, D. L.; Sudesh, K.; Mandal, B. B.; Norma-Rashid, Y.; Oktaviani, N. A.; Preda, R. C.; Pugno, N. M.; Rajkhowa, R.; Wang, X.; Yazawa, K.; Zheng, Z.; Numata, K. 1000 Spider Silkomes: Linking Sequences to Silk Physical Properties. *Sci. Adv.* **2022**, *8* (41), No. eabo6043.

(5) Brunetta, L.; Craig, C. L. Spinning, Running, Jumping, Swimming. In *Spider Silk; Evolution and 400 Million Years of Spinning, Waiting, Snagging, and Mating*; Yale University Press, 2010; pp 96−110.
(6) Candelas, G. C.; Cintron, J. A Spider Fibroin and Its Synthesis. *J. Exp. Zool.* **1981**, *216* (1), 1−6.
(7) Rising, A.; Johansson, J. Toward Spinning Artificial Spider Silk. *Nat. Chem. Biol.* **2015**, *11* (5), 309−315.
(8) Salehi, S.; Scheibel, T. Biomimetic Spider Silk Fibres: From Vision to Reality. *Biochemist* **2018**, *40* (1), 4−7.
(9) Vollrath, F. Strength and Structure of Spiders' Silks. *Rev. Mol. Biotechnol.* **2000**, *74*, 67−83.
(10) Hayashi, C. Y.; Blackledge, T. A.; Lewis, R. V. Molecular and Mechanical Characterization of Aciniform Silk: Uniformity of Iterated Sequence Modules in a Novel Member of the Spider Silk Fibroin Gene Family. *Mol. Biol. Evol.* **2004**, *21* (10), 1950−1959.
(11) Hayashi, C. Y.; Lewis, R. V. Spider Flagelliform Silk: Lessons in Protein Design, Gene Structure, and Molecular Evolution. *BioEssays* **2001**, *23* (8), 750−756.
(12) Sponner, A.; Schlott, B.; Vollrath, F.; Unger, E.; Grosse, F.; Weisshart, K. Characterization of the Protein Components of Nephila Clavipes Dragline Silk. *Biochemistry* **2005**, *44* (12), 4727−4736.
(13) Hu, W.; Jia, A.; Ma, S.; Zhang, G.; Wei, Z.; Lu, F.; Luo, Y.; Zhang, Z.; Sun, J.; Yang, T.; Xia, T.; Li, Q.; Yao, T.; Zheng, J.; Jiang, Z.; Xu, Z.; Xia, Q.; Wang, Y. A Molecular Atlas Reveals the Tri-Sectional Spinning Mechanism of Spider Dragline Silk. *Nat. Commun.* **2023**, *14* (1), No. 837.
(14) Rising, A.; Hjälm, G.; Engström, W.; Johansson, J. N-Terminal Nonrepetitive Domain Common to Dragline, Flagelliform, and Cylindriform Spider Silk Proteins. *Biomacromolecules* **2006**, *7* (11), 3120−3124.
(15) Hagn, F.; Eisoldt, L.; Hardy, J. G.; Vendrely, C.; Coles, M.; Scheibel, T.; Kessler, H. A Conserved Spider Silk Domain Acts as a Molecular Switch That Controls Fibre Assembly. *Nature* **2010**, *465* (7295), 239−242.
(16) Andersson, M.; Chen, G.; Otikovs, M.; Landreh, M.; Nordling, K.; Kronqvist, N.; Westermark, P.; Jörnvall, H.; Knight, S.; Ridderstråle, Y.; Holm, L.; Meng, Q.; Jaudzems, K.; Chesler, M.; Johansson, J.; Rising, A. Carbonic Anhydrase Generates CO2 and H+ That Drive Spider Silk Formation Via Opposite Effects on the Terminal Domains. *PLoS Biol.* **2014**, *12* (8), No. e1001921.
(17) Askarieh, G.; Hedhammar, M.; Nordling, K.; Saenz, A.; Casals, C.; Rising, A.; Johansson, J.; Knight, S. D. Self-Assembly of Spider Silk Proteins Is Controlled by a pH-Sensitive Relay. *Nature* **2010**, *465* (7295), 236−238.
(18) Hagn, F.; Thamm, C.; Scheibel, T.; Kessler, H. pH-Dependent Dimerization and Salt-Dependent Stabilization of the N-Terminal Domain of Spider Dragline Silk - Implications for Fiber Formation. *Angew. Chem., Int. Ed.* **2011**, *50* (1), 310−313.
(19) Kronqvist, N.; Otikovs, M.; Chmyrov, V.; Chen, G.; Andersson, M.; Nordling, K.; Landreh, M.; Sarr, M.; Jörnvall, H.; Wennmalm, S.; Widengren, J.; Meng, Q.; Rising, A.; Otzen, D.; Knight, S. D.; Jaudzems, K.; Johansson, J. Sequential pH-Driven Dimerization and Stabilization of the N-Terminal Domain Enables Rapid Spider Silk Formation. *Nat. Commun.* **2014**, *5*, No. 3254.
(20) Guerette, P. A.; Ginzinger, D. G.; Weber, B. H. F.; Gosline, J. M. Silk Properties Determined by Gland-Specific Expression of a Spider Fibroin Gene Family. *Science* **1996**, *272* (5258), 112−115.
(21) Gatesy, J.; Hayashi, C.; Motriuk, D.; Woods, J.; Lewis, R. Extreme Diversity, Conservation, and Convergence of Spider Silk Fibroin Sequences. *Science* **2001**, *291* (5513), 2603−2605.
(22) Gosline, J. M.; Guerette, P. A.; Ortlepp, C. S.; Savage, K. N. The Mechanical Design of Spider Silks: From Fibroin Sequence to Mechanical Function. *J. Exp. Biol.* **1999**, *202* (23), 3295−3303.
(23) Ayoub, N. A.; Garb, J. E.; Tinghitella, R. M.; Collin, M. A.; Hayashi, C. Y. Blueprint for a High-Performance Biomaterial: Full-Length Spider Dragline Silk Genes. *PLoS One* **2007**, *2* (6), No. e514.
(24) Keten, S.; Xu, Z.; Ihle, B.; Buehler, M. J. Nanoconfinement Controls Stiffness, Strength and Mechanical Toughness of B-Sheet Crystals in Silk. *Nat. Mater.* **2010**, *9* (4), 359−367.
(25) Simmons, A. H.; Michal, C. A.; Jelinski, L. W. Molecular Orientation and Two-Component Nature of the Crystalline Fraction of Spider Dragline Silk. *Science* **1996**, *271* (5245), 84−87.
(26) Liu, R.; Deng, Q.; Yang, Z.; Yang, D.; Han, M. Y.; Liu, X. Y. Nano-Fishnet" Structure Making Silk Fibers Tougher. *Adv. Funct Mater.* **2016**, *26* (30), 5534−5541.
(27) Hayashi, C. Y.; Lewis, R. V. Spider Flagelliform Silk: Lessons in Protein Design, Gene Structure, and Molecular Evolution. *BioEssays* **2001**, *23*, 750.
(28) Kono, N.; Nakamura, H.; Mori, M.; Yoshida, Y.; Ohtoshi, R.; Malay, A. D.; Pedrazzoli Moran, D. A.; Tomita, M.; Numata, K.; Arakawa, K. Multicomponent Nature Underlies the Extraordinary Mechanical Properties of Spider Dragline Silk. *Proc. Natl. Acad. Sci. U.S.A.* **2021**, *118* (31), 1−10.
(29) Rising, A.; Johansson, J. Toward Spinning Artificial Spider Silk. *Nat. Chem. Biol.* **2015**, *11* (5), 309−315.
(30) Ravandi, S. H.; Valizadeh, M. Properties of Fibers and Fabrics that Contribute to Human Comfort. In *Improving Comfort in Clothing*; Woodhead Publishing, 2011; pp 61−78.
(31) Kamalha, E.; Zeng, Y.; Mwasiagi, J. I.; Kyatuheire, S. The Comfort Dimension; a Review of Perception in Clothing. *J. Sens. Stud.* **2013**, *28* (6), 423−444.
(32) Hu, J.; Lu, J. 3 - Recent Developments in Elastic Fibers and Yarns for Sportswear. In *Woodhead Publishing Series in Textiles*; Shishoo, R. B. T., Ed.; Woodhead Publishing, 2015; pp 53−76.
(33) Kluge, J. A.; Rabotyagova, O.; Leisk, G. G.; Kaplan, D. L. Spider Silks and Their Applications. *Trends Biotechnol.* **2008**, *26*, 244−251.
(34) Dellaquila, A.; Greco, G.; Campodoni, E.; Mazzocchi, M.; Mazzolai, B.; Tampieri, A.; Pugno, N. M.; Sandri, M. Optimized Production of a High-Performance Hybrid Biomaterial: Biomineralized Spider Silk for Bone Tissue Engineering. *J. Appl. Polym. Sci.* **2020**, *137* (22), 48739.
(35) Schacht, K.; Vogt, J.; Scheibel, T. Foams Made of Engineered Recombinant Spider Silk Proteins as 3D Scaffolds for Cell Growth. *ACS Biomater. Sci. Eng.* **2016**, *2* (4), 517−525.
(36) Chouhan, D.; Thatikonda, N.; Nilebäck, L.; Widhe, M.; Hedhammar, M.; Mandal, B. B. Recombinant Spider Silk Functionalized Silkworm Silk Matrices as Potential Bioactive Wound Dressings and Skin Grafts. *ACS Appl. Mater. Interfaces* **2018**, *10* (28), 23560−23572.
(37) Mayank; Bardenhagen, A.; Sethi, V.; Gudwani, H. Spider-Silk Composite Material for Aerospace Application. *Acta Astronaut.* **2022**, *193*, 704−709.
(38) Pan, L.; Wang, F.; Cheng, Y.; Leow, W. R.; Zhang, Y. W.; Wang, M.; Cai, P.; Ji, B.; Li, D.; Chen, X. A Supertough Electro-Tendon Based on Spider Silk Composites. *Nat. Commun.* **2020**, *11* (1), 1332.
(39) Blamires, S. J.; Spicer, P. T.; Flanagan, P. J.Spider Silk Biomimetics Programs to Inform the Development of New Wearable Technologies *Front. Mater.* 2020; Vol. *7* DOI: 10.3389/fmats.2020.00029.
(40) Bourzac, K. Spiders: Web of Intrigue. *Nature* **2015**, *519* (7544), S4−S6.
(41) Lefèvre, T.; Auger, M. Spider Silk as a Blueprint for Greener Materials: A Review. *Int. Mater. Rev.* **2016**, *61* (2), 127−153.
(42) Xia, X.-X.; Qian, Z.-G.; Ki, C. S.; Park, Y. H.; Kaplan, D. L.; Lee, S. Y. Native-Sized Recombinant Spider Silk Protein Produced in Metabolically Engineered *Escherichia Coli* Results in a Strong Fiber. *Proc. Natl. Acad. Sci. U.S.A.* **2010**, *107* (32), 14059−14063.
(43) Bowen, C. H.; Dai, B.; Sargent, C. J.; Bai, W.; Ladiwala, P.; Feng, H.; Huang, W.; Kaplan, D. L.; Galazka, J. M.; Zhang, F. Recombinant Spidroins Fully Replicate Primary Mechanical Properties of Natural Spider Silk. *Biomacromolecules* **2018**, *19* (9), 3853−3860.
(44) Li, J.; Zhu, Y.; Yu, H.; Dai, B.; Jun, Y.-S. S.; Zhang, F. Microbially Synthesized Polymeric Amyloid Fiber Promotes *β*-

Nanocrystal Formation and Displays Gigapascal Tensile Strength. *ACS Nano* **2021**, *15* (7), 11843−11853.
(45) Andersson, M.; Jia, Q.; Abella, A.; Lee, X. Y.; Landreh, M.; Purhonen, P.; Hebert, H.; Tenje, M.; Robinson, C. V.; Meng, Q.; Plaza, G. R.; Johansson, J.; Rising, A. Biomimetic Spinning of Artificial Spider Silk from a Chimeric Minispidroin. *Nat. Chem. Biol.* **2017**, *13* (3), 262−264.
(46) Li, X.; Qi, X.; Cai, Y. M.; Sun, Y.; Wen, R.; Zhang, R.; Johansson, J.; Meng, Q.; Chen, G. Customized Flagelliform Spidroins Form Spider Silk-like Fibers at pH 8.0 with Outstanding Tensile Strength. *ACS Biomater. Sci. Eng.* **2022**, *8* (1), 119−127.
(47) Xu, S.; Li, X.; Zhou, Y.; Lin, Y.; Meng, Q. Structural Characterization and Mechanical Properties of Chimeric Masp1/Flag Minispidroins. *Biochimie* **2020**, *168*, 251−258.
(48) Zhou, Y.; Rising, A.; Johansson, J.; Meng, Q. Production and Properties of Triple Chimeric Spidroins. *Biomacromolecules* **2018**, *19* (7), 2825−2833.
(49) Finnigan, W.; Roberts, A. D.; Ligorio, C.; Scrutton, N. S.; Breitling, R.; Blaker, J. J.; Takano, E. The Effect of Terminal Globular Domains on the Response of Recombinant Mini-Spidroins to Fiber Spinning Triggers. *Sci. Rep.* **2020**, *10* (1), 10671.
(50) Chen, J.; Tsuchida, A.; Malay, A. D.; Tsuchiya, K.; Masunaga, H.; Tsuji, Y.; Kuzumoto, M.; Urayama, K.; Shintaku, H.; Numata, K. Replicating Shear-Mediated Self-Assembly of Spider Silk through Microfluidics. *Nat. Commun.* **2024**, *15* (1), No. 527.
(51) Schmuck, B.; Greco, G.; Bäcklund, F. G.; Pugno, N. M.; Johansson, J.; Rising, A. Impact of Physio-Chemical Spinning Conditions on the Mechanical Properties of Biomimetic Spider Silk Fibers. *Commun. Mater.* **2022**, *3* (1), 83.
(52) Arndt, T.; Greco, G.; Schmuck, B.; Bunz, J.; Shilkova, O.; Francis, J.; Pugno, N. M.; Jaudzems, K.; Barth, A.; Johansson, J.; Rising, A. Engineered Spider Silk Proteins for Biomimetic Spinning of Fibers with Toughness Equal to Dragline Silks. *Adv. Funct. Mater.* **2022**, *32* (23), No. 2200986.
(53) Schmuck, B.; Greco, G.; Barth, A.; Pugno, N. M.; Johansson, J.; Rising, A. High-Yield Production of a Super-Soluble Miniature Spidroin for Biomimetic High-Performance Materials. *Mater. Today* **2021**, *50*, 16−23.
(54) Andersson, M.; Jia, Q.; Abella, A.; Lee, X. Y.; Landreh, M.; Purhonen, P.; Hebert, H.; Tenje, M.; Robinson, C. V.; Meng, Q.; Plaza, G. R.; Johansson, J.; Rising, A. Biomimetic Spinning of Artificial Spider Silk from a Chimeric Minispidroin. *Nat. Chem. Biol.* **2017**, *13* (3), 262−264.
(55) Garb, J. E.; Haney, R. A.; Schwager, E. E.; Gregorič, M.; Kuntner, M.; Agnarsson, I.; Blackledge, T. A. The Transcriptome of Darwin's Bark Spider Silk Glands Predicts Proteins Contributing to Dragline Silk Toughness. *Commun. Biol.* **2019**, *2* (1), 275.
(56) Babb, P. L.; Lahens, N. F.; Correa-Garhwal, S. M.; Nicholson, D. N.; Kim, E. J.; Hogenesch, J. B.; Kuntner, M.; Higgins, L.; Hayashi, C. Y.; Agnarsson, I.; Voight, B. F. The Nephila Clavipes Genome Highlights the Diversity of Spider Silk Genes and Their Complex Expression. *Nat. Genet.* **2017**, *49* (6), 895−903.
(57) Elvin, C. M.; Carr, A. G.; Huson, M. G.; Maxwell, J. M.; Pearson, R. D.; Vuocolo, T.; Liyou, N. E.; Wong, D. C. C.; Merritt, D. J.; Dixon, N. E. Synthesis and Properties of Crosslinked Recombinant Pro-Resilin. *Nature* **2005**, *437* (7061), 999−1002.
(58) Chen, G.; Liu, X.; Zhang, Y.; Lin, S.; Yang, Z.; Johansson, J.; Rising, A.; Meng, Q. Full-Length Minor Ampullate Spidroin Gene Sequence. *PLoS One* **2012**, *7* (12), No. e52293.
(59) Fahnestock, S. R.; Irwin, S. L. Synthetic Spider Dragline Silk Proteins and Their Production in *Escherichia Coli*. *Appl. Microbiol. Biotechnol.* **1997**, *47* (1), 23−32.
(60) Nova, A.; Keten, S.; Pugno, N. M.; Redaelli, A.; Buehler, M. J. Molecular and Nanostructural Mechanisms of Deformation, Strength and Toughness of Spider Silk Fibrils. *Nano Lett.* **2010**, *10* (7), 2626−2634.
(61) Bratzel, G.; Buehler, M. J. Sequence-Structure Correlations in Silk: Poly-Ala Repeat of N. Clavipes MaSp1 Is Naturally Optimized at a Critical Length Scale. *J. Mech. Behav. Biomed. Mater.* **2012**, *7*, 30−40.
(62) Hu, C.-F.; Gan, C.-Y.; Zhu, Y.-J.; Xia, X.-X.; Qian, Z.-G. Modulating Polyalanine Motifs of Synthetic Spidroin for Controllable Preassembly and Strong Fiber Formation. *ACS Biomater. Sci. Eng.* **2024**, *10* (5), 2925−2934.
(63) Heidebrecht, A.; Eisoldt, L.; Diehl, J.; Schmidt, A.; Geffers, M.; Lang, G.; Scheibel, T. Biomimetic Fibers Made of Recombinant Spidroins with the Same Toughness as Natural Spider Silk. *Adv. Mater.* **2015**, *27* (13), 2189−2194.
(64) Guerette, P. A.; Ginzinger, D. G.; Weber, B. H. F.; Gosline, J. M. Silk Properties Determined by Gland-Specific Expression of a Spider Fibroin Gene Family. *Science* **1996**, *272* (5258), 112−115.
(65) Kono, N.; Nakamura, H.; Mori, M.; Yoshida, Y.; Ohtoshi, R.; Malay, A. D.; Pedrazzoli Moran, D. A.; Tomita, M.; Numata, K.; Arakawa, K. Multicomponent Nature Underlies the Extraordinary Mechanical Properties of Spider Dragline Silk. *Proc. Natl. Acad. Sci. U.S.A.* **2021**, *118* (31), e2107065118.
(66) Sonavane, S.; Hassan, S.; Chatterjee, U.; Soler, L.; Holm, L.; Mollbrink, A.; Greco, G.; Fereydouni, N.; Vinnere Pettersson, O.; Bunikis, I.; Churcher, A.; Lantz, H.; Johansson, J.; Reimegård, J.; Rising, A. Origin, Structure, and Composition of the Spider Major Ampullate Silk Fiber Revealed by Genomics, Proteomics, and Single-Cell and Spatial Transcriptomics. *Sci. Adv.* **2024**, *10* (33), No. eadn0597.
(67) Blackledge, T. A.; Hayashi, C. Y. Silken Toolkits: Biomechanics of Silk Fibers Spun by the Orb Web Spider Argiope Argentata (Fabricius 1775). *J. Exp. Biol.* **2006**, *209* (13), 2452−2461.
(68) Kono, N.; Ohtoshi, R.; Malay, A. D.; Mori, M.; Masunaga, H.; Yoshida, Y.; Nakamura, H.; Numata, K.; Arakawa, K. Darwin's Bark Spider Shares a Spidroin Repertoire with Caerostris Extrusa but Achieves Extraordinary Silk Toughness through Gene Expression. *Open Biol.* **2021**, *11* (12), No. 210242.
(69) Wen, R.; Wang, S.; Wang, K.; Yang, D.; Zan, X.; Meng, Q. Complete Gene Sequence and Mechanical Property of the Fourth Type of Major Ampullate Silk Protein. *Acta Biomater.* **2023**, *155*, 282−291.
(70) Gaar, J.; Naffa, R.; Brimble, M. Enzymatic and Non-Enzymatic Crosslinks Found in Collagen and Elastin and Their Chemical Synthesis. *Org. Chem. Front.* **2020**, *7* (18), 2789−2814.
(71) Qiu, W.; Huang, Y.; Teng, W.; Cohn, C. M.; Cappello, J.; Wu, X. Complete Recombinant Silk-Elastinlike Protein-Based Tissue Scaffold. *Biomacromolecules* **2010**, *11* (12), 3219−3227.
(72) Gonzalez-Obeso, C.; Backlund, F. G.; Kaplan, D. L. Charge-Modulated Accessibility of Tyrosine Residues for Silk-Elastin Copolymer Cross-Linking. *Biomacromolecules* **2022**, *23* (3), 760−765.
(73) Xia, X. X.; Xu, Q.; Hu, X.; Qin, G.; Kaplan, D. L. Tunable Self-Assembly of Genetically Engineered Silk-Elastin-like Protein Polymers. *Biomacromolecules* **2011**, *12* (11), 3844−3850.
(74) Weis-Fogh, T. Molecular Interpretation of the Elasticity of Resilin, a Rubber-like Protein. *J. Mol. Biol.* **1961**, *3* (5), 648−667.
(75) Michels, J.; Appel, E.; Gorb, S. N. Functional Diversity of Resilin in Arthropoda. *Beilstein J. Nanotechnol.* **2016**, *7*, 1241−1259.
(76) Balu, R.; Dutta, N. K.; Dutta, A. K.; Choudhury, N. R. Resilin-Mimetics as a Smart Biomaterial Platform for Biomedical Applications. *Nat. Commun.* **2021**, *12* (1), 149.
(77) Zhao, S.; Ye, X.; Dai, X.; Wang, X.; Yu, S.; Zhong, B. Drosophila Melanogaster Resilin Improves the Mechanical Properties of Transgenic Silk. *PLoS One* **2023**, *18* (3), No. e0282533.
(78) Kono, N.; Nakamura, H.; Ohtoshi, R.; Moran, D. A. P.; Shinohara, A.; Yoshida, Y.; Fujiwara, M.; Mori, M.; Tomita, M.; Arakawa, K. Orb-Weaving Spider Araneus Ventricosus Genome Elucidates the Spidroin Gene Catalogue. *Sci. Rep.* **2019**, *9* (1), 8380.
(79) Leppert, A.; Chen, G.; Lama, D.; Sahin, C.; Railaite, V.; Shilkova, O.; Arndt, T.; Marklund, E. G.; Lane, D. P.; Rising, A.; Landreh, M. Liquid−Liquid Phase Separation Primes Spider Silk Proteins for Fiber Formation via a Conditional Sticker Domain. *Nano Lett.* **2023**, *23* (12), 5836−5841.

https://doi.org/10.1021/acsomega.4c06031
ACS Omega 2024, 9, 42423−42432

(80) Malay, A. D.; Suzuki, T.; Katashima, T.; Kono, N.; Arakawa, K.; Numata, K. Spider Silk Self-Assembly via Modular Liquid-Liquid Phase Separation and Nanofibrillation. *Sci. Adv.* **2024**, *6* (45), No. eabb6030.
(81) Gabryelczyk, B.; Sammalisto, F.-E.; Gandier, J.-A.; Feng, J.; Beaune, G.; Timonen, J. V. I.; Linder, M. B. Recombinant Protein Condensation inside *E. Coli* Enables the Development of Building Blocks for Bioinspired Materials Engineering − Biomimetic Spider Silk Protein as a Case Study. *Mater. Today Bio* **2022**, *17*, No. 100492.
(82) Fan, R.; Knuuttila, K.; Schmuck, B.; Greco, G.; Rising, A.; Linder, M. B.; Aranko, A. S. Sustainable Spinning of Artificial Spider Silk Fibers with Excellent Toughness and Inherent Potential for Functionalization. *Adv. Funct. Mater.* **2024**, *26*, No. 2410415.
(83) Madurga, R.; Plaza, G. R.; Blackledge, T. A.; Guinea, G. V.; Elices, M.; Pérez-Rigueiro, J. Material Properties of Evolutionary Diverse Spider Silks Described by Variation in a Single Structural Parameter. *Sci. Rep.* **2016**, *6* (1), 18991.
(84) Schmuck, B.; Greco, G.; Pessatti, T. B.; Sonavane, S.; Langwallner, V.; Arndt, T.; Rising, A. Strategies for Making High-Performance Artificial Spider Silk Fibers. *Adv. Funct. Mater.* **2023**, No. 2305040.
(85) Greco, G.; Schmuck, B.; Jalali, S. K.; Pugno, N. M.; Rising, A. Influence of Experimental Methods on the Mechanical Properties of Silk Fibers: A Systematic Literature Review and Future Road Map. *Biophys. Rev.* **2023**, *4* (3), 031301.

https://doi.org/10.1021/acsomega.4c06031
ACS Omega 2024, 9, 42423−42432